Advanced Compact Models for MOSFETs

Josef Watts[1](editor), Colin McAndrew[2](presentor),Christian Enz[3], Carlos Galup-Montoro[4],
Gennady Gildenblat[5], Chenming Hu[6], Ronald van Langevelde[7], Mitiko Miura-Mattausch[8],
Rafael Rios[9], Chih-Tang Sah[10]

[1]IBM Corp., [2]Freescale Semiconductor, [3]Ecole Polytechnique Fédérale de Lausanne, [4]Universidade Federal de Santa Catarina, [5]Dept. of Electrical Engineering, The Pennsylvania State University, [4]Dept. of Electrical and Computer Engineering, University of California, Berkeley, [7]Philips Research [8]Advanced Sciences of Matter, Hiroshima University, [9]Intel Corporation, [10]University of Florida,

ABSTRACT

The combination of decreasing MOSFET dimensions and increasing use of MOSFETs for analog and RF application has created the need for advanced compact models for MOSFET circuit design. The first generation of MOSFET models rely on approximate solutions that are only valid in particular regions of operation connected mathematically to provide continuous solutions. This leads to inaccuracy between regions and therefore inaccuracy in simulating circuits where those regions are important to the circuit function. This paper provides an overview of the basic physics that must be modeled to build a compact model for the MOSFET and describes the approaches taken by the developers of several advanced models.

Keywords: compact model, surface potential model, charge based model, mosfet model

1 INTRODUCTION

The MOSFET is inherently a two-dimensional (2-D) electronic device. Its input voltage is applied in the x-direction perpendicular to a semiconductor surface in order to modulate the current which flows near the surface in the y-direction when a voltage is applied to the two ends of the device. The first step in creating an analytic model is a device-physics-based decomposition of the 2-D problem into two 1-D problems. [1] The 1-D x-solution is known as the **input voltage equation**, which relates applied gate voltage to the electric conditions of the semiconductor surface. This is an electrostatic solution of Poisson's equation. The 1-D y-solution is known as the **output current equation**, which relates the current passing between the drain and source to the x-solution and the voltages applied to the source and drain. This solution involves conduction down the channel by the mechanisms of drift and diffusion. This separation of the problem is called the gradual channel approximation because it requires assuming that the potential along the channel varies gradually enough for the 1-D electrostatic solution to be valid.

Pao and Sah [2] obtained a solution in the form of a double integral (over the thickness of the inversion layer and the length of the channel). Evaluation requires numerical integration and is too computation intensive for use in a compact model. However the so called Pao-Sah

equation is highly physical and still serves as a reference to test the accuracy of less computation intensive solutions. The next step in the development of MOS models was the use of the charge-sheet approximation [3,4,5], which assumes the inversion layer is infinitesimally thin i.e. the potential does not vary through the thickness of the channel. This yields implicit not explicit expressions for the surface potential in terms of the applied voltages. Given the computing power available at the time early SPICE models needed a simpler solution to the input voltage equation.

The solution adopted was the threshold voltage (V_T) based formulation which assumes the surface potential is a very simple function of the input voltage: constant for V_g above V_T and a linear function of gate voltage below V_T. This results in separate solutions for different regions of MOSFET operation requiring smoothing functions to connect the regions. These functions can be deduced from experiment [6]. Despite their limitations such models have been successfully used for much circuit design work. BSIM4 and MOS Model 9 are modern versions of threshold voltage based models.

Other MOSFET models can be divided into two groups based on the approach they take to solving the **input and output equations.** One approach is to solve for the input equation surface potential at the two ends of the channel. The terminal charges, currents and derivatives are then calculated from the surface potential. These models are called surface potential models. Four of the present authors are involved with development of such models. (Gildenblat—SP, van Langevelde—MOS Model 11, Miura-Mattausch—HiSIM and Rios—A Practical Source-Side Only Model).

Another approach is to find the density of the inversion charge at the two ends of the channel and formulate the model outputs in terms of these charge densities. We will call these "charge based models" meaning that both conductance and capacitance calculations are based on charge (all models in this paper explicitly calculate terminal charges). Other terms have been used including "inversion charge based", "charge control" and "unified" models. Three of the present authors are involved with the development of such models. (Enz—EKV, Galup-Montoro—ACM and Hu—BSIM5)

After selecting an approach to solving the fundamental differential equations the model developer faces many more

challenges due to the non-ideal real devices. These include complex doping profiles and small dimensions that lead to a variety of physical effects. As devices evolve models must evolve to keep up. In the following sections model developers describe some of the large and small choices that shape seven particular advanced MOSFET models.

2 CHARGE BASED MODELS

A practical compact model requires efficient and accurate algorithms to calculated currents, charges and derivatives. Maher and Mead [7] showed that the drain current can be expressed as a function of the area densities of the inversion charge at the source and the drain. Cunha et al. [8] derived expressions for the total charges and small signal parameters as a function of the source and drain channel charge densities. Shur's group proposed the Unified Charge Control Model [9] and introduced, without derivation [10], an equation for the charge densities as a function of terminal voltages. Gummel et al. [11] recently provided a theoretical derivation for basically the same charge equation and proposed a charge-based model called USIM. He, et al. [12] provided an alternate derivation of a similar charge solution. These models rely on the gradual channel and charge sheet assumptions and a linearization of the bulk and inversion charges with respect to the surface potential at a fixed gate bias. For the accumulation region (where there is no inversion charge) several approaches are possible. A equation similar to that for inversion charge can be derived for the accumulation charge or a surface potential based approach, among others can be used.

2.1 The ACM Model

The MOS modeling activities of the S. Catarina University group, beginning in the late 80´s, were motivated by their work at that time on analog design in digital CMOS technology. The use of the MOS gate as a linear capacitor required the calculation of the weak nonlinearities of the MOS capacitor in accumulation and strong inversion. The classical strong inversion (SI) approximation was clearly not appropriate and improved capacitive models of the MOS gate valid for moderate inversion (MI) and accumulation were therefore developed [13]. The use of the new gate capacitor model to achieve a four terminal MOS model accurate in SI and MI, was a natural step forward [14]. The model [14] used lengthy surface potential based expressions for current and charges and was not satisfactory for analog design. The need for a symmetrical MOSFET model [15] to describe the series association of transistors became clear at that time [16].

An appropriate MOSFET model was finally achieved in [8]. The symmetry of the transistor with respect to source and drain was obeyed. Explicit expressions for the current, charges, transconductances and the 16 capacitive coefficients valid in weak, moderate and strong inversion were made available. All transistor parameters were given as very simple (rational) functions of the inversion charge densities at the channel boundaries.

The model in [8] was based on two physical features of the MOSFET structure: the charge-sheet model [3] and the incrementally linear relationship between the inversion charge density Q'_I and the surface potential Φ_S [7]

$$dQ'_I = nC'_{ox}d\Phi_S$$
$$n = 1 + C'_b / C'_{ox} \tag{1}$$

In (1), C'_{ox} is the oxide capacitance per unit area and C'_b is the depletion capacitance calculated assuming the inversion charge to be negligible. n is the slope factor, slightly dependent on the gate voltage.

A link between the charge model of [8] and the current-based model of [15] was obtained in [17, 18].

Dc, ac and non-quasi-static models were developed in [18,19]. Rigorous definitions of pinch-off and threshold voltages, essential to consistent and precise models, were given as follows.

The channel charge density for which the diffusion current equals the drift current is designated the **pinch-off charge density Q'_{ip}**

$$Q'_{ip} = -nC'_{ox}\varphi_t \tag{2}$$

where φ_t is the thermal voltage

The channel-to-substrate voltage (V_C) for which the channel charge density equals Q'_{ip} is called the **pinch-off voltage V_P**. The **equilibrium threshold voltage V_{TO}**, measured for $V_C=0$, is the gate voltage for which the channel charge density equals Q'_{ip}.

The unified charge control model (UCCM) [9,10] was theoretically derived in [20] adding a new basic approximation to the model in [8]. Considering the inversion capacitance C'_i proportional to the inversion charge it follows [20] that:

$$dQ'_I\left(\frac{1}{nC'_{ox}} - \frac{\varphi_t}{Q'_I}\right) = dV_C \tag{3}$$

Integrating (3) between an arbitrary channel potential V_C and the pinch-off voltage V_P, yields the UCCM.

A computer-implemented version of the model, called ACM (Advanced Compact MOSFET), has been included in a circuit simulator since 1997 [21]. ACM has a hierarchical structure that facilitates the inclusion of different phenomena into the model [22]. Because of its very simple expression for the derivative of the channel charge density (3), ACM was the first, and is still the only model to furnish simple explicit expressions for all the intrinsic capacitive coefficients, even when short channel effects [22] are taken into account. Parameters of the ACM model can be easily extracted, as shown in [18, 20]. Recently, unified 1/f noise and mismatch models were presented in [23, 24]

2.2 The EKV Model

The EKV model was initially developed for the design of very low-power analog ICs, with the objective of having

a simple analytical model valid in all modes of inversion. It was important to correctly handle the weak inversion part since many micropower circuits were designed based on the MOS transistor operating in this region [25]. The first paper about EKV [26] [1] already exploited the symmetry of the device by referring all the terminal voltages to the substrate. It also redefined the forward and reverse currents initially proposed for strong inversion in [27] extending it to all modes of inversion. The fundamental concept of normalized forward current (also called inversion factor) and reverse current were also defined and used for circuit design optimization. The moderate inversion region was covered by an empirical interpolation function after proper normalization. Even though this early model used the linearization of the inversion charge with respect to the channel voltage to derive the drain current, it was actually not a charge-based model at this stage. It was rather based on a continuous g_m /I characteristics, following the intuition that the transconductances are proportional to the inversion charge. It was only latter that a physical function covering weak to strong inversion could be derived [28, 29, 30], following the pioneering work of Maher [7, 31], giving rise to the charge-based EKV model. A rigorous derivation of the charge-based EKV model and a detailed modeling of the inversion charge linearization can be found in [32].

Referencing the voltages to the bulk not only preserves and exploits the symmetry of the device in the model, but also allows to clearly distinguish between effects that do not affect this symmetry property, such as all the effects related to the transverse field (mobility reduction due to the transverse field, poly depletion [33], quantum effect [34], non-uniform doping in the transverse direction [35]) and the effects related to the longitudinal direction such as velocity saturation, non-uniform doping in the longitudinal direction, that destroy the symmetry property [36]. An additional feature of the symmetrical model is that the effects related to the transverse field can be modeled by using the basic equations after properly pre-warping the parameters.

From a designer's point of view, the most relevant parameters are often the transconductances. From the basic physics of the MOS transistor, it turns out that the source and drain transconductances are actually proportional to the inversion charge density Q_i evaluated at the source Q_{iS} and at the drain Q_{iD} respectively. It can be shown that the normalized chages $q_s = Q_{iS}$ /Q_{spec} and $q_d = Q_{iD}$ /Q_{spec} where $Q_{spec} = -2nC_{ox}\varphi_T$ q_s and q_d not only determine the transconductances, but actually all the important MOST variables, including the current [37,38], the terminal charges [39], the capacitances [39], the transcapacitances [39,40,41], the admittances [40,41], the transadmittances [40,41], and the thermal noise, including the induced-gate noise [42,43,44]. The normalized charges q_s and q_d are depending on the terminal voltages according to [37, 38]

---

[1] The EKV name originates from the initials of the authors of this paper.

$$v_p - v_{s(d)} = 2q_{s(d)} + \ln q_{s(d)} \qquad (4)$$

where voltages are normalized with the thermal voltage and charge densities are normalized as $q_i = Q_i$ /$(-2nC_{ox}\varphi_t$) The charge-based modeling approach allows therefore decoupling the relations between the variables mentioned above and the terminal voltages by using the intermediate q_s and q_d variables [45].

Although EKV is a charge-based model, the inversion charge linearization gives a direct relation between the surface potential Φ_s and the inversion charge density Q_i according to [37, 38].

$$\Phi_s = \Phi_P - \left(-Q_i\right)/nC_{ox} \qquad (5)$$

where Φ_P is a function of the gate voltage only and is defined as the value of Φ_s for which $Q_i = 0$. The pinch-off voltage is then computed as $V_P = \Phi_P - 2\Phi_F - m\,\varphi_T$, where m can be considered as constant and typically ranging between 2 and 4 [32]. The definition of Φ_P applies initially in depletion and inversion, but in the EKV approach, Φ_P (V_G) is formulated to also cover the accumulation region. This is illustrated in Fig. 1 where the surface potential is calculated from the inversion charge according to (5) and compared to the result obtained from numerical simulations.
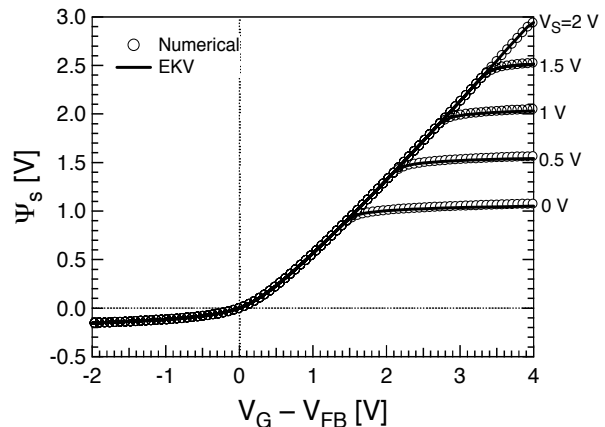

Figure 1: Approximation of the surface potential from the inversion charge according to (5).

The EKV charge-based model has now evolved into a full featured scalable compact model that includes all the major effects that have to be accounted for in deep submicron CMOS technologies [46, 47, and 48]. The recently released EKV version 3.0 features a coherent physical and hierarchical description of all the static, dynamic and noise aspects, while retaining a reduced number of parameters 46, 47, 48]. The EKV model is currently being extended to double-gate device architectures using the EKV charge-based approach [49]. More informations about the EKV model can be found at [50].

2.3 The BSIM5 Model

In both surface potential and charge based models an implicit function needs to be evaluated to find the surface potential in one case or the charge density in another for each set of bias voltages in SPICE iterations. Since the current is an exponential function of the surface potential but a linear/quadratic function of the charge density, the calculation of the charge density need not to be carried out to as high a degree of accuracy as the surface potential.

BSIM5 uses a single set of equations to calculate charges throughout all the bias regions. It can relatively easily incorporate short-channel, non-uniform doping, and numerous other effects to accurately model subtle details of the device behaviors in the tradition of BSIM4. Special attention is paid to higher-order physics such as accurate current saturation and quantum mechanical effect. It is fully symmetric and smooth.

Assuming gradual channel and constant quasi-Fermi level, I_{ds} can be expressed as a product of the gradient of the quasi-fermi potential V_{ch} and the inversion charge density Q_i as:

$$I_{ds} = \mu_{eff} W Q_i \frac{dV_{ch}}{dy} \tag{6}$$

The inversion charge density (normalized with $q_I = Q_I/(\varphi_t C_{ox})$ and $v = V/\varphi_t$) can be expressed as:

$$\ln\left(\frac{q_I}{n}\right) + \frac{q_I}{n} = \frac{v_{GB} - v_{FB}}{n} - \varphi_B - v_{ch} - n\ln\left(\frac{n}{n-1}\right) \tag{7}$$

where n is the slope factor. Combining Eq(6-7) and then integrating from source to drain results in:

$$I_{ds0} = \frac{\mu w}{L} C_{ox} \left(\frac{kT}{q}\right)^2 \left[\frac{q_s^2 - q_d^2}{2n} + (q_s - q_d)\right] \tag{8}$$

The inversion charge densities at the source and drain (q_s and q_d) can be calculated from (7). Fig.2. shows that BSIM5 accurately models the inversion charge density.
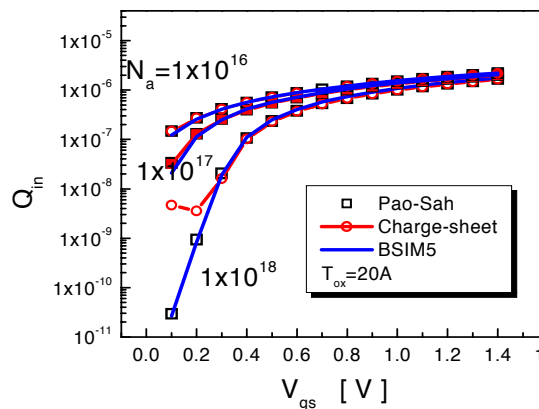
Fig.2 Comparison of charge among BSIM5, the charge-sheet model [54] and the Pao-Sah model[2]

Poly-depletion and the quantum effects are partially included in (8), which also models more detailed physics with additional terms in BSIM5. Velocity saturation, velocity overshoot and source-velocity limit are modeled in a unified way. BSIM5 shows (Fig.3) that the classical velocity saturation underestimates the drain current for 45nm technology while the hydrodynamic model overestimates the current because source-velocity limit starts to take effect.

BSIM5 core model can be easily extended to model non-classical devices such as ultra-thin-body SOI and multi-gate devices including FinFET[50].
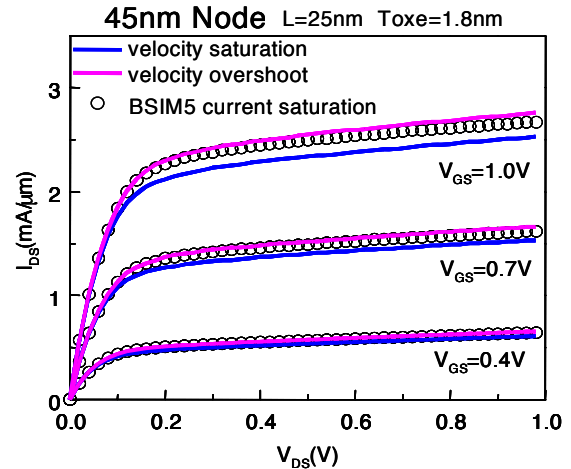
Fig. 3 BSIM5's predictive unified current saturation model.

3 SURFACE POTENTIAL MODELS

Until relatively recently Φ_s-based models were often considered too complicated for the compact modeling purposes. One major reason for this was that, techniques for computation of the surface potential were not developed sufficiently. Applying the gradual channel and charge sheet assumptions yields an implicit relation for the surface potential in terms of the applied voltages[2,3]. The published iterative schemes to solve this equation were relatively slow and did not include all regions of the operation. Non-iterative approximations did not extend to the accumulation region and were not sufficiently accurate especially (as noted in [51]) for the purpose of computing the transcapacitances. It is important to note that in the 1980's the structure of the dominant V_T-based models was still relatively simple so that the penalty associated with the iterative computation of Φ_s was believed (at that time!) to be non-trivial.

Today the computation of the surface potential is no longer an issue. Considerable progress has been made in the development of the iterative algorithms [52,53,54,55] some of which obtain an accuracy of 10 pV with no more than 2 iterations for most bias conditions. Non-iterative analytical approximations have also been developed [56, 57] some of which can deliver an accuracy of better than 1 nV except (at least for the published work) in the cases of the extreme

forward bias of the source-substrate junctions [52, 59]. As a result the time required to evaluate Φ_s is about 5-10% of the total execution time for surface potential models. It has been demonstrated that the surface-potential-based model can be faster than some state-of-the art Vt based models [55].

One other drawback of the original Φ_s-based models [3, 60] was their use of complex and lengthy expressions for currents, charges and noise [61]. To simplify these calculations surface potential models developed more efficient approaches. One method is a linearization of the inversion charge as a function of the surface potential.

3.1 A Practical Source-Side Only Model

Practical and efficient surface potential MOSFET models can be derived based on a source-side only surface potential solution. One such model, inspired from the original work of Park [62], was developed in 1995 [63] and used in DEC's Alpha chip design from 1996. The model was also extended for SOI devices in 1996, featuring automatic and physical transitions between partially- and fully-depleted modes of operations [64].

The source-side only solution represents a good compromise between accuracy and the simplicity and solution speed required for practical applications. The approach not only avoids solving for the surface potential on the drain side, but also results in a simple and self-consistent treatment of carrier velocity saturation. In addition, appropriate treatment of the body charge linearization and the effective drain bias can be used to maintain source/drain symmetry. Some of the key core model assumptions and approximations, necessary to build an accurate and efficient source-side only approach, are highlighted here.

The mobile carrier charge density q_i, required for the integration of the current continuity equation, is obtained from charge conservation: $q_i = - (q_g + q_b)$. From Gauss' law, the gate charge density is accurately given by

$$q_g = C_{ox}\left(V_{gb} - V_{fb} - \Phi_S\right) \tag{9}$$

A good approximation for the body charge density is given by (10), valid for all regions of operation, unlike the simplified form (11), which is invalid in accumulation. The even simpler form (12), often employed for q_i calculations, is invalid even in weak accumulation as can be seen in fig. 4.

$$q_b = -\text{sign}\left(\Phi_S\right)C_i\gamma\sqrt{\Phi_S + \varphi_t\left(e^{-\Phi_S/\varphi_t} - 1\right)} \tag{10}$$

$$q_b = -C_i\gamma\sqrt{\Phi_S + \varphi_t} \tag{11}$$

$$q_b = -C_i\gamma\sqrt{\Phi_S} \tag{12}$$

To obtain simple analytic solutions, especially for terminal charges, q_b needs to be converted into a linear function of Φ_s. A simple endpoints linearization can be obtained by evaluating (10) at the source, Φ_{ss}, and drain, $\Phi_{sd} = \Phi_{ss} + V_{dsx}$, ends of the channel, where V_{dsx} is the effective drain voltage. The endpoints linearization has the nice features of maintaining accurate q_b values at the source and drain endpoints as well as preserving source/drain symmetry.
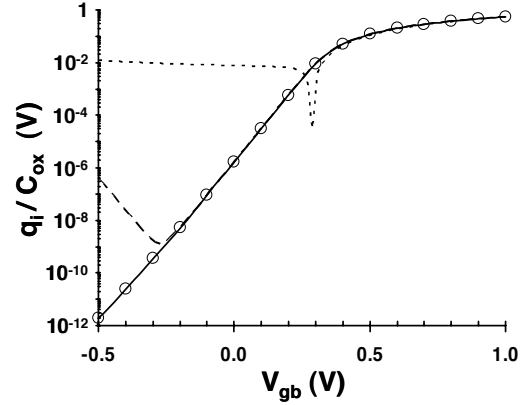

Fig 4: Inversion charge density calculated with (10), full line, (11), dashed line, and (12), doted line. Circles are results from full numerical solutions of the Poisson equation.

A good approximation for the effective drain voltage V_{dsx} was proposed in [65]. However, for the source-side only solution approach, the function $\Phi_{sd} = \Phi_{ss} + V_{dsx}$ would not capture the correct behavior of ϕ_{sd} for small V_{ds}. This can be fixed by obtaining the correct derivative g = $d\Phi_s/dV_{ds}$ for $V_{ds} \rightarrow 0$ directly from the surface potential equation. V_{dsx} is forced to match this derivative using the expression:

$$V_{dsx} = gV_{ds}\left[1 + \left(gV_{ds}/V_{dsat}\right)^m\right]^{-1/m} \tag{13}$$

In addition to preserving source/drain symmetry, (13) produces the correct drain current behavior near $V_{ds} = 0$.

For models that rely on the drain side surface potential solution, self-consistent and efficient handling of the carrier velocity saturation effect on Φ_{sd} has been a difficult problem to solve [65, 66], usually increasing the model complexity. One of the main advantages of the source-side only approach is that simple, explicit, and self-consistent V_{dsat} solutions are possible by equating the saturation drain current to the model drain current equation, at $V_{dsx} = V_{dsat}$.

The velocity-field relation requires special treatment to be able to include the effect of longitudinal field dependent mobility in the integration of the continuity equation. A good approximation was proposed in [67], with the additional benefit of preserving source/drain symmetry, as recently pointed out in [68].

The lateral field gradient [69], an attractive approach to treat small geometry effects, was evaluated for the practical model of [63]. However, it was abandoned due to limitations on the maximum threshold voltage roll-off of $\Delta V_T < \gamma \, (2\Phi_f - V_{bs})^{1/2}$ for the surface potential relation to have physical solutions, as well as inconsistent impact on the sub-threshold slope. Instead, and similarly to standard V_T-based models, the source-referenced Φ_s-based approach allows treatment of threshold voltage shifts due to small geometry and non-uniform doping effects as simple shifts in gate overdrive. The short-channel V_T model of [70], with simple corrections to maintain source/drain symmetry, gives excellent results. Longitudinal doping non-uniformity can be modeled as in [71].

A simple linear analytic solution for the gate field reduction due to poly-depletion can be used to integrate the effect along the channel [72]. Quantum mechanical effects on the inversion charge density can be handled in a physical manner by a band-gap widening approach [63].

3.2 The HiSIM Model

Early efforts have been given to develop practical circuit simulation models based on the drift-diffusion concept and proved its feasibility for real applications [54, 55]. They have been practically applied the development of DRAM, medical system ICs and IC-card products at Siemens since 1993. In recent years the potential of surface-potential approach was widely realized and received a lot of additional attention and development efforts [73-75]. In the surface-potential-based modeling, the surface potential is the measure of all device characteristics, which are very much dependent on technology. HiSIM (Hiroshima-university STARC IGFET Model) obtains the potentials by solving the Poisson equation iteratively both at the source side and drain side. An accuracy of 10 pV has been achieved with faster simulation time than some threshold voltage based models [55]. Such an extreme accuracy turned out to be absolutely necessary for maintaining sufficient accurate solutions for transcapacitance values as well as to achieve stable circuit simulation.

An important task, which had to be completed before applying the surface-potential-based modeling to advanced MOSFETs, was the derivation of a method for incorporating the short-channel effect. For this purpose, the Poisson equation has to be solved in principle in two dimensions. The first approach had been to solve the equation with double looped iteration. However, it was realized that the effect can be reduced to the inclusion of the gradient of longitudinal electric field. In this way the short-channel effect could be derived analytically as the threshold voltage shift, and could be included in a quasi 1-dimensional Poisson equation. This approach originated with [76] was first applied to compact modeling in [77] using geometry-dependent lateral field gradient approximation. To derive further analytical equations required for circuit simulation, different approaches have

been investigated. The resulting MISNAN model [66] introduces a parabolic potential distribution along the channel. On the other hand, HiSIM implements charge and capacitance equations which maintain the gradual-channel approximation and provide a solution in the saturation condition by extending the surface potential beyond the pinch-off point [78]. Simulated surface potential values by HiSIM are shown in Fig. 5. Once the surface-potential values at source and drain side are known, all device characteristics are calculated without any additional parameter. Since this is the core approach of the surface-potential-based modeling and at the same time the core of the device physics, a 1-to-1 correspondence between circuit-simulation model and device physics is readily obtainable.
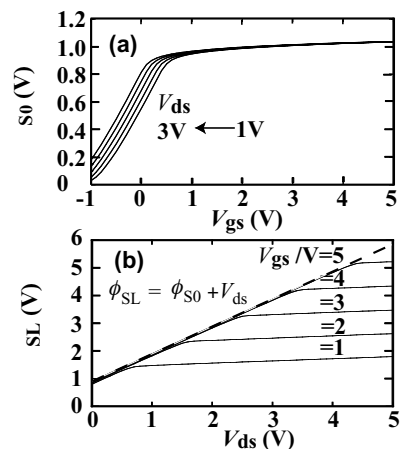

Fig. 5: Simulated surface potential values with HiSIM at (a) source side as a function of Vgs, and (b) drain side as a function of Vds. The short-channel effect is incorporated in the values.

For advanced MOSFETs, the surface-potential distribution along the channel determines the MOSFET features, and that the surface-potential distribution is determined by MOSFET parameters such as the bulk impurity profile. Intensive MOSFET-channel engineering is being undertaken to extend the application of the MOSFET-technology to the nano-technology era. Thus accurate modeling of the effects of such advanced technologies is a very important part of the surface-potential-based modeling and has been the subject of recent researches. The modeling of the pocket implantation, for example, in HiSIM is done by taking into account the pocket profile precisely [79]. A 1-dimensional analytical description could be achieved by approximating a linearly graded profile. This pocket-implantation model has been verified to be predictable and as accurate as 2D-simulation results. Such modeling approach automatically preserves scalability of model parameters, and thus, one model-parameter-set for all device dimensions is no question for HiSIM.

A big advantage of a complete surface-potential-based model is that the overall model consistency is automatically preserved through the surface potential. Therefore, the

number of model parameters can be drastically reduced in comparison with conventional models [55]. This parameter reduction comes without any loss in reproduction accuracy of measurement data as e.g. the I-V characteristics. Moreover, it has been verified that the non-linear phenomena such as harmonic distortion are automatically accurately calculated [80]. All higher-order phenomena observed such as noise have been shown to be determined by the potential gradient along the channel [81, 82], which again highlights the strength of the concept of surface-potential-based modeling. Investigations of the high-frequency small-signal behavior with HiSIM concluded that the non-quasi-static effect is not as strong as previously believed [83]. In summary, it can be concluded that without considering the surface-potential distribution along the channel, modeling should become unnecessarily complicated and inaccurate.

3.3 MOS Model 11

MOS Model 11 (MM11) is the successor to MOS Model 9 [84]. Its development started in 1994, and aimed at fulfilling the following demands:

- Accurate, physical description of all MOSFET operation regions including the moderate inversion region and the accumulation region for varactor modelling;
- Computational complexity should allow application in digital designs;
- Accuracy should satisfy demands from analogue and RF circuit design. Analogue and RF design typically require an accurate description of not only currents and capacitances, but also of the small-signal, distortion and noise behaviour.
- Accurate description of all important physical effects of modern and future technologies; and
- A simple parameter extraction methodology.

MM11 fulfils all of the above demands. In the following, we will briefly discuss how MM11 has been developed within the general context of compact MOS modelling.

Surface potential models use a single expression for drain current and give a physics-based and accurate description in all operation regions including the moderate inversion and the accumulation region. As discussed above the charge based model and the V_T-based model are special simplified cases of the Φ_s-based model. The ψ_s-based model thus has the most general form, and as a result it is the natural choice for an advanced MOS model such as MM11.

To obtain efficient expressions for model outputs, several approximations were developed mainly based on a linearization of the inversion charge as a function of ψ_s. In MM11, a linearization is performed around the average of source and drain surface potentials [85, 86], which results in simpler expressions without a loss of accuracy. A different linearization approach (such as a linearization around the source-side surface potential as is done in V_T-

based models), may lead to wrong results in certain circuit applications such as, e.g., the R2R circuit [87]. In addition, the MM11 approach also ensures that the model symmetry with respect to source-drain interchange is maintained. Note that this approach is not unlike the symmetric linearization method used in SP [88], which made it easy to merge the best features of MM11 and SP into one model called PSP.

Finally, we note that, with the above linearization approach, a Φ_s-based model forms an excellent basis for an easy implementation of well-known physical phenomena such as, e.g., thermal noise [89], new phenomena appearing in new applications such as, e.g., induced gate noise [89], or new phenomena appearing in new technologies such as, e.g., gate leakage [90]. For each of these examples MM11 contains original contributions.

The original Φ_s-based charge-sheet models describe the electrical behaviour of an ideal long-channel MOSFET. For the description of realistic devices, however, the model has to be extended with an accurate description of mobility effects and conductance effects. In MM11, these effects have been added with a special emphasis on distortion modelling.
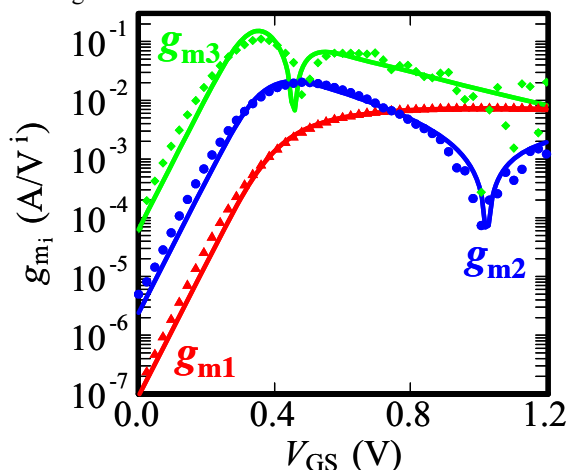

Fig. 6: MM11 gives an accurate description of distortion behaviour. Measured (symbols) and modelled (lines) higher-order derivatives g_{mi} ($=\partial^i I_D/\partial V_{GS}^i$) as a function of gate bias V_{GS} for W/L=10μm/0.1μm device. (n-MOS, V_{DS}=0.73V, V_{SB}=0V)

For an accurate description of distortion, the model should accurately describe the drain current and its higher-order derivatives (up to at least 3rd-order). MM11 has especially been developed for this purpose. As a result, compared to other models, MM11 contains improved expressions for mobility reduction [91], velocity saturation and various conductance effects [92]. The distortion modelling of MM11 has been extensively tested on various MOSFET technologies [93], and it gives an accurate description of modern CMOS technologies, see Fig. 6. A special case of distortion modelling concerns the model

symmetry with respect to source-drain interchange. Model asymmetry leads to discontinuities in the higher-order derivatives of channel current at V_{DS}=0 [73]. In MM11, care has been taken to preserve symmetry in the model expressions [87, 91] as illustrated in fig. 6.

With respect to symmetry, it should be pointed out here that symmetrical and asymmetrical models are often mistakenly identified as bulk-referenced and source-referenced, respectively [94]. Bulk-referencing is no guarantee for a model to be symmetrical, while a source-referenced model can be perfectly symmetrical, e.g., MM11 (see also [91]). As a consequence, it is misleading to categorize compact models in source-referenced and bulk-referenced models, and it makes more sense to talk about symmetrical and asymmetrical models.

For modern CMOS technologies several physical effects have become important that did not affect circuit design before. All these effects should be described by the compact MOS model. MM11 includes an accurate description of all important physical effects, such as poly-depletion [95], quantum-mechanical effects [95], the effect of pocket implants [96], gate tunnelling current [55], bias-dependent overlap capacitances [95], gate-induced drain leakage and noise [54].

Finally, it should be mentioned that the model structure of MM11 is different from any other model. In MM11, a distinction is made between local parameters, which are parameters valid for a device with a specific geometry, and global parameters, which are parameters valid for all devices with different geometries in one technology. The model equations make use of local parameters, and the local parameters can be written in terms of the instance parameters (e.g., W, L) and the global parameters. MM11 can be addressed on a local level and on a global level separately, which allows for a rigorous separation of model equations (i.e., currents and charges in terms of applied bias) and geometry scaling relations (i.e., local parameters in terms of geometry). This facilitates model development and a simple parameter extraction.

3.4 The SP Model

In the development of SP we have selected the surface potential based structure for the following reasons. It is the most general form from which the others follow as special cases. Since in our formulation [97] the equations of the Φ_s–based model are as simple as those in Vt or q_i - based models there is almost no price to pay for this generality and relatively high physical content. The fundamental advantage of the Φ_s –based approach is that it allows one to use a single set of equations for all regions of operation Similarly, only this approach allows one to physically model the source-drain overlap regions where the threshold voltage or inversion charge cannot be used.

The double–integral formula of [2] can be easily extended to include low-temperature operation and transverse field-dependent mobility [98] and can be transformed into a somewhat more efficient form by careful variable transformation [99]. The development of Φ_s-based

compact models was initiated very soon after the work of Brews [3]. All of the existing Φ_s-based models use the charge-sheet approximation as a starting point. We note in passing that while the original charge-sheet model did not include the accumulation region this omission is not catastrophic and is easily rectified in the modern versions [97, 59]. In [100,101] some short-channel effects were introduced and the need to describe the saturation region differently than in [1, 3] (where velocity saturation was not included) was recognized. Accurate non-iterative technique has been developed for computing the surface potential (including the case of the lateral field gradient) [103]. A simpler but equally accurate non-iterative solution for Φ_s exists for the source-drain overlap regions where the minority carriers can be neglected [102]. With different physical interpretation this algorithm is also useful in the dynamic varactor models [104] and in the NQS model [105]. Since the majority carriers are not affected by the imref splitting, the substrate forward bias is not an issue in this case.

In a surface potential model short-channel effects can no longer be accounted for by simply adding new terms to the expression for the threshold voltage. This problem has been gradually solved in the modern Φ_s-based models by accumulating the necessary experience and trying different approaches. For example, the SP formulation goes beyond the gradual channel approximation by using the bias and geometry dependent lateral gradient factor originally introduced in [76]. The geometry depend version was already used in [77]. The last problem that, for a while, retarded the development of the Φ_s-based models was their relatively complicated structure, especially of the expressions for the intrinsic charges. For the original charge-sheet model these were computed in [106], and subsequently in [107,108] in an explicit form. These complicated expressions are not suitable for the purpose of compact modeling so various approximations were developed based, primarily, on the linearization of the inversion charge as a function of the surface potential. The technique used in SP was influenced by the observation in [73] that this linearization is a critical step that when done improperly may bring about a violation of the Gummel symmetry test and consequential difficulties in the simulation of passive mixers and related circuits [68]. The symmetric linearization method developed in SP [58,97,108] preserves the Gummel symmetry and produces expressions for both the drain current and the terminal charges that are as simple as those in Vt-based or q_i-based models (e.g. no fractional powers like 3/2 often associated with the charge-sheet model) and are numerically indistinguishable from the original charge-sheet model equations [58,108]. As a result SP is at least as fast as the latest Vt-based models. We note in passing that the symmetric linearization approach is not particularly sensitive to the details of the velocity saturation model which is enabling the merger of the best features of the SP

and MM11 models (the PSP model presented in a companion paper in this volume).

The charge linearization relative to the source is not the only cause responsible for the violation of the Gummel symmetry test. As pointed out in [73, 68] the other problem is the singular nature of the popular velocity saturation model

$$v_d = \mu_0 |E| \Big/ \left(1 + \left(|E| / E_c \right)^n \right)^{1/n} \tag{14}$$

with n=1. In the above equation E_c denotes the critical field and μ_0 is the effective channel mobility for low longitudinal field E. The problem can be solved using n=2 (cf. the related formulation in [86]) or by adopting a V_{ds} dependent critical field originally introduced in compact modeling for a different purpose [109, 67]. When combined with the symmetric linearization method this technique automatically solves the singularity issue [68, 97].

Some of the specific features of SP include its unique symmetric linearization method, completely non-iterative formulation, non-regional description from accumulation to strong inversion, inclusion of all relevant short-channel and thin-oxide effects, bias-dependent effective doping to deal with "halo" effects, physical description of the overlap regions and of the "inner-fringing" effects, and the comprehensive and accurate NQS model based on the spline collocation method [108]. The latter has been recently extended to include the accumulation region [105] and the small-geometry effects. Finally, we note that when combined with the general one-flux theory of the non-absorbing barrier SP [110, 111] is capable of reproducing the quasi-ballistic effects using the one-flux method [112].

4 Conclusions

Two approaches to MOSFET compact models have been described. The future direction for the industry is unclear. We hope this paper and the forum at the 2005 WCM of which the paper is a part provide some facts and perspective to help light the way. The GEIA Compact Model Council is currently examining examples of both types and their work will provide additional insight into the consequences of various modeling choices. Ultimately engineers responsible for providing models to meet the needs of circuit designers will decide which model to use.

References

[1] Chih-Tang Sah, Fundamentals of Solid-State Electronics, 1001pp, 1991, World Scientific Publishing Company, Singapore
[2] H. C. Pao and C. T. Sah, SSE, vol. 9, p. 927, 1966.
[3] J.R. Brews, SSE, Vol. 21, p.345, 1978.
[4] F. van de Wiele, SSE, Vol. 22, pp. 991, 1979.
[5] G. Baccarani, et al., IEE J. Solid-State and Electron Devices, vol. 2, pp.62, 1978.
[6] Y. Cheng et al, IEEE TCAD, pp. 641, 1998
[7] M. A. Maher and C. A. Mead, Advanced Research in VLSI,. Cambridge, MA: MIT Press, 1987.
[8] A. I. A. Cunha, et al., SSE, vol. 38, p. 1945, Nov.1995.
[9] Y. Byun, K. Lee and M. Shur, IEEE Electron Device Letters, vol. 11, p. 50, Jan. 1990.
[10] C.-K. Park, et al., IEEE TED, vol. 38, p. 399, 1991
[11] H. K. Gummel and K. Singhal, IEEE TED, vol. 48, p. 1585, 2001
[12] J. He et al., Proc. MSM 2003
[13] A. T. Behr, et al., IEEE Journal of Solid-State Circuits, vol. 27, p. 1470, Oct.1992.
[14] A. I. A. Cunha, et al., in Proc. Brazilian Microelectronics Conf . (SBMICRO 93), 1993.
[15] C. C. Enz, PhD Thesis no. 802, EPF-Lausanne, Switzerland, 1989.
[16] C. Galup-Montoro, et al., IEEE J. Solid-State Circuits, V. 29, p. 1094, 1994.
[17] C. Galup-Montoro, et al., Proc. Brazilian Micro-electronics Conf . (SBMICRO 96), pp. 287-292, 1996.
[18] A. I. A. Cunha, M. C. Schneider, and C. Galup-Montoro, IEEE JSSC, V 33, p. 1510, 1998.
[19] C. Galup-Montoro, M. C. Schneider, and A. I. A. Cunha, Chapter 2 of Low-Voltage/Low-Power Integrated Circuits and Systems, p. 7, IEEE Press, 1999.
[20] A. I. A. Cunha, et al., SSE, V 43, p. 481, March 1999.
[21] Application Notes in Home-page Dolphin, http://www.dolphin.fr/medal/smash/notes/acm_report.pdf
[22] O. C. Gouveia Filho, et al., IEEE CICC, p. 209, 2000.
[23] A. Arnaud and C. Galup-Montoro, IEEE TED, V 50, p. 1815, 2003.
[24] C. Galup-Montoro, et al. in WCM 2004, Boston.
[25] E. Vittoz and J. Fellrath, IEEE JSSC, V 12, p. 224, 1977.
[26] C. C. Enz, et al., Analog Integrated Circuits and Signal Processing Journal, V 8, p. 83, 1995.
[27] J.-D. Châtelain, Dispositifs à Semiconducteur, vol. VII, 2nd ed, Editions Georgi, 1979.
[28] A. I. A. Cunha, et al., Proc. IEEE Int. Symp. Circuits Syst., p. 1608, 1997.
[29] M. Bucher, et al., Proc. of the Int. Semiconductor Device Research Symp., 1997.
[30] H. K. Gummel and K. Singhal, IEEE TED, V 48, p. 2384, Oct. 2001.
[31] C. Mead, in Analog VLSI and Neural Systems, Addison-Wesley, 1989.
[32] J.-M. Sallese, et al., SSE,Vol. 47, p. 677, 2003.
[33] J.-M. Sallese, et al., SSE, Vol. 44, p. 905, 2000.
[34] C. Lallement, et al., IEEE TED, Vol. 50, p. 406, 2003.
[35] C. Lallement, et al., SSE, V 41, p. 1857, 1997.
[36] E. Vittoz, et al., Proc. WCM, p. 246, 2003.
[37] J.-M. Sallese and A.-S. Porret, SSE, V 44, p. 887, 2000.
[38] J.-M. Sallese, et al., Proc. of the 8th Int. Conf. on Mixed Design of Integrated Circuits and Systems (MIXDES), 2001.
[39] M. Bucher, et al., Proc. of the Int. Semiconductor Device Research Symp., pp. 397-400, 1999.
[40] A.-S. Porret, et al., IEEE TED,Vol. 48, p. 1647, 2001
[41] C. Enz, IEEE Trans. Microwave Theory Tech., Vol. 50, p. 342, 2002.

[42] A.-S. Porret and C. C. Enz, IEE Proc.-Circuits Devices Syst., Vol. 151, p. 155, 2004.

[43] A. S. Roy and C. C. Enz, Proc. of the 11th Int. Conf. on Mixed Design of Integrated Circuits and Systems, p. 71, 2004.

[44] A. S. Roy and C. C. Enz, Submitted to IEEE TED, 2005.

[45] C. C. Enz, et al., WCM, p. 666, 2002.

[46] M. Bucher, et al., WCM, p. 670-, 2002.

[47] M. Bucher, et al., Proc. of the 9th Int. Conf. on Mixed Design of Integrated Circuits and Systems (MIXDES), pp. , June 2002.

[48] M. Bucher, to be presented at the WCM, May 2005.

[49] J.-M. Sallese, et al., SSE, vol. 49, pp. 485-489, 2005.

[50] http://legwww.epfl.ch/ekv/

[51] C.-H. Lin et al., to be published at VLSI-TSA – TECH, April 25-27, 2005 Hsinchu, Taiwan.

[52] M. Bagetti and Y.P. Tsividis, IEEE TED V 32, p. 2383, 1985

[53] R. Rios et al., IEDM Tech. Digest, pp. 755-758, 2004.

[54] M. Miura-Mattausch et al., Proc. VPAD, 98, 1991; IEICE Trans. Electron., E75-C, 172, 1992

[55] M. Miura-Mattausch, et al., Tec. Digest ICCAD, pp. 264-267, 1994; M. Miura-Mattausch, et al., IEEE Trans. CAD/ICAS, 15, 1, 1996.

[56] R. van Langevelde, et al., Proc. WCM, p. 60, 2004.

[57] R. van Langevelde and F.M. Klaassen, SSE, Vol. 44, pp. 409-418, 2000.

[58] G. Gildenblat and T.-L. Chen, SSE, Vol. 45, pp. 335-341, 2001.

[59] W. Wu, et al, IEEE TED, 51, 1196 2004

[60] F. van de Wiele, SSE, Vol. 22, pp. 991-997, 1979.

[61] C.C. McAndrew and J.J. Victory, IEEE TED, ED-49, 72, 2002.

[62] H. Park et al., IEEE T-CAD, pp. 376-389, 1991.

[63] R. Rios et al., IEDM Tech. Digest, pp. 937-940, 1995.

[64] J. W. Sleight et al., IEDM Tech. Dig., 143, 1996.

[65] K. Joardar, et al., IEEE TED, pp. 134-148, 1998.

[66] A.R. Boothroyd, et al., IEEE TCAD., Vol. CAD-10, pp. 1512-1529, 1991.

[67] N. D. Arora et al., IEEE TED, pp. 988-997, 1994.

[68] P. Bendix, et al., IEEE CICC 2004, p. 9-12.

[69] M. Miura Mattausch, IEEE T-CAD, p. 610, 1994.

[70] Z. Liu et al., IEEE TED, p. 86, 1993.

[71] R. Rios, et al., IEDM Tech. Digest, p. 113, 2002.

[72] N. D. Arora, IEEE TED, p. 935, 1995.

[73] K. Joardar, et al., IEEE TED, V. 45, p. 134, 1998.

[74] R. van Langevelde, et al., Proc. MSM, p. 674, 2002.

[75] G. Gildenblat and T. –L. Chen, Proc. MSM, p. 657, 2002.

[76] T. Nguen and J. Plummer, IEDM Tech. Digest, 1981, p. 596

[77] M. Miura-Mattausch and H. Jaocobs, Jpn J. Appl. Phys., vol. 29, pp. L2279-2282, 1990.

[78] M. Miura-Mattausch, et al., IEIEC Trans. Fundamentals, V. E85-A, 740, 2002.

[79] D. Kitamaru, et al., Proc. SISPAD, pp. 392-395, 2001;

H. Ueno, et al., IEEE TED, vol. 49, pp. 1783-1789, 2002.

[80] S. Chiba, et al., Applied Physics Meeting, 28p-ZL-4, 2003.

[81] S. Matsumoto, et al., IEIEC Trans. Electron., vol. E88-C, 2005.

[82] S. Hosokawa, et al., Ext. Abs. SSDM, 20, 2003.9.

[83] H. Ueno, et al., Proc. SISPAD, pp. 71-74, 2002.9.

[84] R.M.D.A. Velghe, et al., NL-UR 003/94, Philips Electronics N.V., 1994.
www.semiconductors.philips.com/Philips_Models

[85] R. van Langevelde, Ph.D. Thesis, TU Eindhoven, Eindhoven, 1998.

[86] R. van Langevelde, et al. NL-TN 2003/00239, Philips Electronics N.V., 2003.
www.semiconductors.philips.com/Philips_Models

[87] D.B.M. Klaassen, et al. IEICE Trans. Electron., Vol. E87-C, pp. 854-866, 2004.

[88] T.-L. Chen and G. Gildenblat, Electron. Lett., V 37, p. 791, 2001.

[89] R. van Langevelde, et al. IEDM Tech. Dig., p. 867, 2003.

[90] R. van Langevelde, et al. IEDM Tech. Dig., p. 289, 2001.

[91] R. van Langevelde and F.M. Klaassen, IEEE TED, V ED-44, p. 2044, 1997.

[92] R. van Langevelde and F.M. Klaassen, IEDM Tech. Dig., pp. 313-316, 1997.

[93] R. van Langevelde et al., IEDM Tech. Dig., pp. 807-810, 2000.

[94] W. Liu, IEEE Circuits & Devices, Vol. 18, p. 29, 2002.

[95] R. van Langevelde, et al. Proc. ESSDERC, p. 81, 2001.

[96] A.J. Scholten, et al. Proc. ESSDERC, pp. 311, 2001.

[97] G. Gildenblat, et al, IEEE JSSC, 39, 1392, 2004

[98] C.-L. Huang and G. Gildenblat, SSE, 36, 611, 1993

[99] M. Persi and G. Gildenblat, SSE, 38, 1461, 1995

[100] C. Turchetti and G. Masetti, IEEE JSSC, 21, 267, 1984

[101] H.-J. Park, et al, IEEE TCAD, 10, 376 (1991)

[102] X. Gu, et al., IEEE TED, 51, 127 (2004)

[103] T.L. Chen and G. Gildenblat, SSE 45, 335 (2001); SSE 49, 267 (2005)

[104] J. Victory, et al., IEEE TED (in press)

[105] H. Wang and G. Gildenblat, Proc. 2004 IEEE CICC p. 5

[106] C. Turchetti, G. Masetti, and Y. Tsividis, SSE, 26, 941(1983)

[107] C.C. McAndrew and J.J. Victory, IEEE TED, 49, 72 (2002)

[108] H. Wang, et al., IEEE TED, 50, p2262, 2003

[109] T. Grotjohn and B. Hoefflinger, IEEE TED, 31, 109 (1984)

[110] G. Gildenblat, J. Appl. Phys., 91, 9883 (2002)

[111] H. Wang and G. Gildenblat, 2002 IEDM Tech. Dig., p. 15

[112] M. Lundstromand Z. Ren, IEEE TED, 49,133 (2002)